Spectral Structure of Turbulent Fluxes in the Atmospheric Boundary Layer over a Thermally Non-Homogeneous Land Surface - with a small summary of GAME related ABL studies –

*** Tetsuya HIYAMA[1], Mikhail A. STRUNIN[2], Michiaki SUGITA[3], and Joon KIM[4]**
(1: HyARC, Nagoya University, Japan, 2: Central Aerological Observatory, Russia, 3: University of Tsukuba, Japan, 4: Yonsei University, Korea)
*** HyARC, Nagoya University, Furo-cho, Chikusa-ku, Nagoya 464-8601, Japan**
e-mail: hiyama@hyarc.nagoya-u.ac.jp

Abstract

This presentation consists of two parts. As a first step in the presentation, a statistical result on the recent research topics in the atmospheric boundary layer (ABL) community is shown. The number of research papers focusing on ABL and turbulent structures over several non-homogeneous land surfaces is increasing and published recently.

Next we introduce one of the important research results on the ABL and turbulent structures over a non-homogeneous land surface, obtained from GAME related sub-project. Data obtained during aircraft observations in convective boundary layer (CBL), developed over thermally well-marked patch with mesoscale size on a land surface, were the basis for the spectral analysis of airflow. Research was conducted at a Lena River site near Yakutsk City from April to June 2000, as part of GAME-Siberia experiments. Analysis of wavelet cospectra and spectra allowed separating fluxes and some other variables into turbulent (with the scales less than depth of CBL or approximately 2 km) and mesoscale (up to 20 km) to explore them independently. Analyses showed that vertical distributions of turbulent and mesoscale portions of the fluxes (sensible heat, water vapour, momentum and carbon dioxide fluxes) and other variables (wind speed and air temperature fluctuations) obeyed different laws. Turbulent vertical scaling profiles of all fluxes followed an almost hyperbolic decay, which differed from generally accepted similarity models for the CBL. Mesoscale vertical profiles of all fluxes and other variables clearly showed sharp inflections at the same relative height of 0.55 in the CBL. Our findings suggest that conventional similarity models for sensible heat fluxes describe both turbulent and mesoscale flows. The peculiarities of vertical profiles supported the suggestion that different kinds of mesoscale motions existed in the mixed layer. The results indicate that the motion that expanded up to the relative (with respect to the depth of the CBL) level of 0.55 could have been initiated by thermal surface heterogeneity. Entrainment processes between the upper part of the CBL and the free atmosphere may have caused the other mesoscale motion.

Keyword: Aircraft observation, Non-homogeneous land surface, Turbulent and mesoscale characteristics, Wavelet transform

1. Introduction

1.1. Overview of recent ABL studies

The number of ABL-related papers was statistically reviewed. We selected four major international journals mainly dealing with ABL studies e.g., “Boundary-Layer Meteorology (BLM)”, “Journal of Applied Meteorology (JAM)”, “Journal of Geophysical Research (D-series; Atmosphere) (JGR)”, and “Agricultural and Forest Meteorology (AFM)”. As a result, research papers focusing on ABL and turbulent structures over several non-homogeneous land surfaces, including urban canopy, land-sea interfacial region, and thermally heterogeneous land surface, are published frequently. The number of papers focusing on cloud-topped boundary layer (CTBL), and those on formations of ABL in some mesoscale meteorological conditions using data set of aircraft observations and Large-Eddy Simulations (LESs) is also increasing recently.

1.2. ABL studies in GAME-Siberia based on aircraft observation

From the statistical reviews described above, we recognized that ABL structures over heterogeneous surface or CTBL are important issues to be studied recently. We introduce one of the important research results on the ABL and turbulent structures over a non-homogeneous land surface, obtained from GAME related sub-project.

The study was conducted as part of GAME-Siberia aircraft observations made during the so-called Intensive Observation Period from April to June 2000 (IOP2000), in the vicinity of Yakutsk City, Eastern Siberia. Previous analyses determined the development of a mesoscale thermal internal boundary layer (MTIBL) inside the CBL over the Lena River and its banks (Strunin et al., 2004). The present paper examines the wavelet spectral analyses of fluxes and discusses how different-sized eddies have contributed to energy, water vapour, and carbon dioxide throughout the CBL.

2. Observation site and flight schemes

Details of aircraft observations during the IOP2000 in the vicinity of Yakutsk City were provided in Hiyama et al. (2003). We used data from research flights undertaken at approximately one-week intervals (depending on weather conditions) on May 1, 9, 12, and 20 and on June 1, 5, 9, and 19, 2000.

The sampling site near Yakutsk consisted of two riverbanks of the Lena River. Long flight paths between the banks crossed the Lena River lowlands approximately perpendicular to the main channel of the river. These flights were termed as “regional” sampling legs or paths. Regional flight paths of about 90 km in the east-west direction were made at five different levels above the highest point of the underlying terrain.

Measurements on the regional flight paths were taken

from around 1200 to 1330 local solar time (i.e., in the middle of the day, when temporal variations in surface fluxes should not be large).

The surface under the flight paths can be characterized as non-homogeneous. The surface state and the state of the Lena varied with the seasons. Both the size of the heterogeneous underlying surface, and the temperature contrast between the river lowland and the surrounding terrace, changed with the season.

Total depth of CBL z_i is applied as a vertical scale above surface layer. Changing of z_i was apparent in a local decrease of the upper CBL boundary over the Lena River and its lowlands. Thus, a local depth of the CBL $\delta(x)$ was defined as a function on the distance along the regional flight path x as;

$$\delta_i = \frac{1}{L_{max}} \int_0^{L_{max}} \delta(x)dx \qquad (1)$$

where L_{max} is the total distance of the regional flight path. Values of δ_i were used in scaling equations instead of the main depth of the CBL z_i, and all scaling profiles were built up versus the normalised (or relative) height z/δ_i (z is the height above the underlying surface).

3. Wavelet analysis

A wavelet transform was applied for spectral analysis of the turbulent variables $f(t)$ or $g(t)$ and turbulent fluxes in the CBL. A detailed description and investigation of this method is presented in Strunin and Hiyama (2004).

Turbulence characteristics derived from aircraft turbulence data are usually calculated using length a and wave number k. According to Taylor's hypothesis, time t was converted to distance b as $b=Ut$, and frequency ξ was converted to wave number k as $k=\xi/U$. The wavelet transform was applied to a spatial-scale function $f(x)$ as follows:

$$Wf(a,b) = \frac{1}{|a|^{1/2}} \int_{-\infty}^{+\infty} f(x)\Psi\left(\frac{x-b}{a}\right)dx \qquad (2)$$

where $a=1/k$ is the spatial scale of the turbulent eddy, and b is the distance along the flight path (or location).

The wavelet spectrum was calculated as follows (Hudgins et al., 1993);

$$S_f(a) = C_\Psi^{-1} \int_{-\infty}^{+\infty} |Wf(a,b)|^2 db \qquad (3)$$

where C_Ψ is the normalising coefficient (C_Ψ=1.0636). A wavelet cross-spectrum (Hudgins et al., 1993) was also calculated as follows.

$$S_{fg}(a) = C_\Psi^{-1} \int_{-\infty}^{+\infty} Wf(a,b)\overline{Wg(a,b)}db \qquad (4)$$

Investigations have shown the reliability of the wavelet method using the present data set (Strunin and Hiyama, 2004). Good coincidence of the Morlet wavelet with the Fourier spectra for small-scale turbulent eddies has been shown. Comparison of the Morlet and Haar wavelet spectra has also shown good results for the large-scale part of the spectra.

4. Results

Wavelet cospectra between vertical wind speed fluctuations and potential temperature fluctuations, humidity fluctuations, carbon dioxide fluctuations were calculated according to equation (4). As well known, wavelet transform executes strong smoothing cospectra at small wave numbers. This is one of important features of the wavelet method, which made it the most suitable for the spectral analysis of atmospheric turbulence. In order to smooth curves at long wavelengths cospectra were smoothed with a five-points moving average filter. Then cospectra were normalised based on maximum absolute values of correspondent line-averaged fluxes.

4.1. Separation of cospectra into turbulent and mesoscale parts

Normalised wavelet cospectra versus the normalised (non-dimensional) wave number kz for flight experiments from 1 May to 19 June were plotted. As the results, almost all obtained cospectra had two clearly expressed peaks, indicating the existence of exchange mechanisms with two prevailing scales. We suggest that the smaller-scale peak characterises turbulent motion and the larger-scale peak corresponds to mesoscale flow. Clearly expressed peaks in the cospectra indicated that two types of motion induced fluxes of substances in the CBL. The first type consisted of turbulent eddies with scales less than the reduced depth of the CBL δ_i. Peaks in this part of the cospectra were most evident for normalised cospectra in sensible heat and carbon dioxide fluxes. The second type consisted of mesoscale flows with a scale ranging from δ_i (about 2 km) up to 20 km. We assumed that these distributions could be decomposed into two Gaussian curves. Figure 1 shows the procedure for separating cospectra into turbulent and mesoscale parts. The wave number axis is presented in a logarithmic scale.

We considered four typical situations. The curve of the calculated cospectrum is presented as dependent on the wave number by a logarithmic scale, and is shown by the solid black line. The dotted grey line shows the turbulent part, and the grey solid line marks the mesoscale part of the cospectrum. In the clearest case, when mesoscale and turbulent peaks of the cospectrum are far from each other (scales differ by 5 – 10 times), the minimum of the cospectrum can be chosen as the boundary between the parts (Figure 1a**,** boundary shown with the line A - B). This situation was typical for numerous cospectra. If mesoscale and turbulent peaks had opposite directions, the point of the change in the cospectra sign was treated as the boundary between the two types of motion. If there were close peaks (Figure 1b) or distant peaks (Figure 1c), the difference was not considered essential. These situations were most typical for carbon dioxide cospectra. If cospectra peaks were close to one another (scales differed by less than five times, as illustrated in Figure 1d), we applied other separation techniques. Solid and dotted grey lines in this panel demonstrate the mesoscale and turbulent distributions of fluxes. To find the point of separation, we constructed a tangent line in the bend of the curve between peaks. The 45^o inclination of the tangent line corresponded to the crossing point of additive Gaussian distributions, which we treated as the separation point between the mesoscale and turbulent parts of the fluxes. This situation was typical for water

vapour cospectra.

Thus, all cospectra (solid black curves) can be treated as a combination of two independent distributions: the right-hand one (dashed grey curves) corresponds to the turbulent part, and the left-hand one (solid grey curves) corresponds to the mesoscale part. Turbulent and mesoscale fluxes are shown by squares under the dashed and solid grey curves, respectively (Figure 1a).

Thus, we presented cospectra as superposition of two kinds of motion, which could be explored separately. This allowed deriving the different relations for "pure" turbulent and mesoscale portions of fluxes.

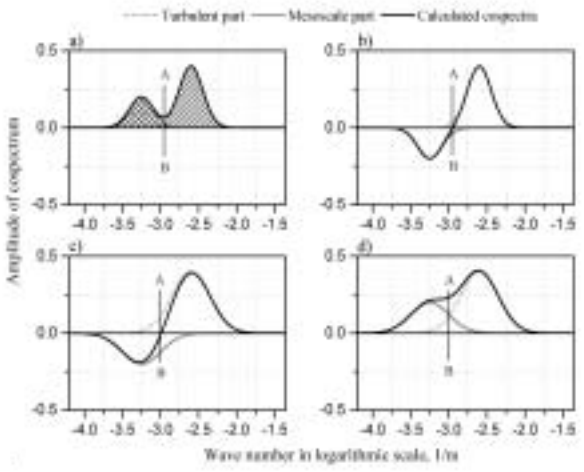

Figure 1. Scheme of separating the mesoscale and turbulent parts of cospectra for their different combinations. Lines A – B in panels show the scale boundaries between mesoscale and turbulent parts of cospectra.

4.2. Scaling of turbulent and mesoscale fluxes

Decomposition of cospectra allowed the separating and independent scaling of the "pure" turbulent and mesoscale portions of sensible heat, water vapour, momentum, and carbon dioxide fluxes. Turbulent and mesoscale parts of the fluxes were calculated through integrating cospectra at corresponding scale ranges. As mentioned above, cospectrum estimated through the cospectra showed practically full coincidence with flux calculated by the eddy correlation method (Strunin and Hiyama, 2004). Boundaries between turbulent and mesoscale parts were defined separately for each sampling path, but they were the same for different kinds of fluxes.

Results of flux scaling based on data obtained for all regional sampling paths (experiments from May 1 to June 19, 2000) are presented in Figure 2**.** Height was normalised on corresponding reduced depths of the CBL δ_i. Typical values of 95% confidential intervals, estimated based on random error are also shown in the figure. As Figure 2 clearly shows, turbulent and mesoscale flux profiles behaved differently for all kinds of fluxes. Turbulent sensible heat fluxes decreased with height and became negligibly small near the upper boundary of the CBL. Scattering of points is very small, suggesting hyperbolic dependence on height. Scattering of the normalised momentum and water vapour turbulent fluxes was larger, but these fluxes also decreased with height and became small at the top of the CBL. In any case scattering of the profile points did not exceed 95% confidential intervals. Depending on surface conditions, turbulent carbon dioxide flux can be upward or downward and its average value (which used as shift in scaling the fluxes) changes in wide limits. Presence of sinks and sources on underlying surface prevents the vanishing of the fluxes to the upper part of CBL. Nevertheless, the shape of the scaled flux profile was similar to those for other turbulent fluxes. Thus, it is possible to say that turbulent carbon dioxide flux behaved analogously to other turbulent fluxes, but with respect to some reference (non-zero) value of the flux.

Vertical profiles of the mesoscale parts of all fluxes (right-hand side panels in Figure 2) are essentially different from corresponding turbulent fluxes. All profiles had peculiarity (a strong inflection) at the same normalised height of approximately z/δ_i = 0.55 (marked by dashed lines in the right-hand side panels of Figure 2). This inflexion exceeds 95% confidential interval, thus it can be treated as reliable. Sensible heat fluxes were almost constant up to this height and had values of 0.2 – 0.4 of the total fluxes. However, at the highest levels, or at normalised heights more than 0.55 the fluxes decreased rapidly and became negative (downward flux) at a normalised height range of 0.7 – 0.8. Profile of mesoscale fluxes of water vapour also has strong inflection at the normalised height of 0.55. The behaviour of carbon dioxide mesoscale profile is similar to the mesoscale parts of other fluxes.

Hyperbolic decay of the turbulent sensible heat fluxes contradicts generally accepted similarity models of the CBL (see, for example, Kaimal and Finnigan, 1994; Sorbjan, 1991). As it seen from Figure 2, total sensible heat flux profiles could be created by summarising the turbulent and mesoscale portions of the fluxes. The resulting profile has a shape that is close to that of the conventional similarity model. Flux decreased with the height and became zero at a normalised height z/δ_i of approximately 0.7 – 0.8. Downward fluxes were strongest at the top of the CBL. This behaviour is typical of the flux profile of a CBL over a homogeneous land surface. More detailed consideration shows that sensible heat flux profile does not strictly obey general accepted model. The profile bends at the normalised height of around 0.1 – 0.2 (due to the large values of turbulent fluxes), and again at a height of approximately 0.5 – 0.6 (due to the strong blending of mesoscale flux profiles). It is important to note that Albertson and Parlange (1999) predicted this shape of the flux profile over an arid heterogeneous patched surface based on a large eddy simulation (LES) technique (see Fig. 2 in Albertson and Parlange, 1999). The quality coincidence of theoretical and experimental results validates the reliability and efficiency of the applied separation approach.

Mesoscale flows in the upper and lower parts of the CBL had different natures. The role of mesoscale motion increased with height and maximised in the middle part of the mixed layer. Mesoscale exchanges then sharply decreased, and increased again at the higher level. In our

opinion, the presence of two peaks in the profiles indicates that there were two mechanisms of mesoscale exchange in the non-homogeneous CBL. One was caused by the influence of a thermally heterogeneous land surface. This influence extended up to the middle of the CBL (z/δ_i = 0.55). Another mechanism was constituted by the entrainment process between the CBL and the free atmosphere or, in the case of MTIBL development, the entrainment process between the upper part of the layer and zones above that layer. Thus, we suggest that the influence of surface-level thermal mesoscale heterogeneity extended only up to the normalised height of z/δ_i = 0.55, where these motions then died out. The next loop of the vertical profile was determined by entrainment from the free atmosphere (in a case without MTIBL development) or the zone above the MTIBL. The space above the zone of MTIBL development cannot be treated as free atmosphere, but rather as a vast area of entrainment (Strunin et al., 2004).

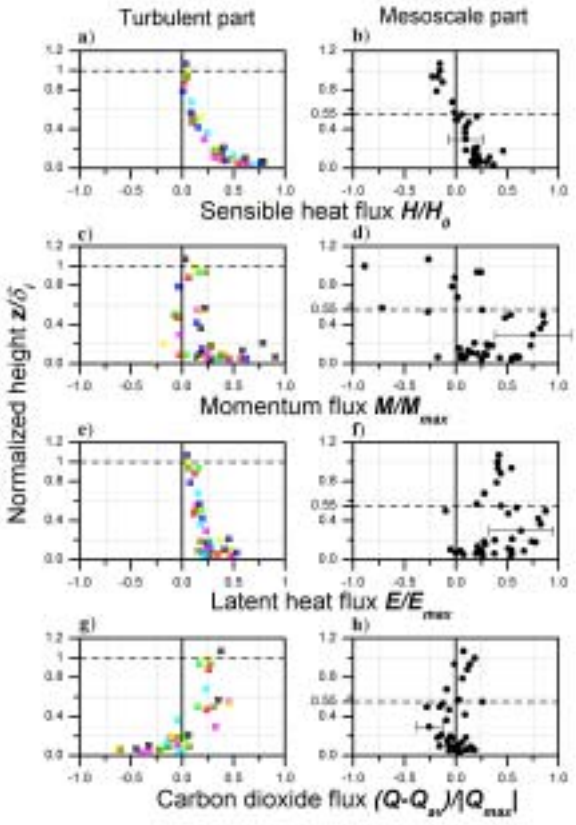

Figure 2. Scaling of mesoscale and turbulent parts of sensible heat *H*, momentum *M*, water vapour *E* and carbon dioxide *Q* fluxes based on correspondent absolute maximum fluxes.

5. Conclusions

Wavelet transform was applied for the aircraft data obtained over the land surface with thermally-mesoscale size of path surfaces. The wavelet transform gave potentiality to investigate spectral characteristics of non-homogeneous variables and overlap practically full-scale range of airflow in the CBL. This technique also allowed correctly separating flows in the CBL into turbulent (with the scale length less than the depth of the CBL, i.e., approximately 1 – 2 km) and mesoscale motions to a maximum scale of 20 km. Clearly expressed peaks in wavelet cospectra and spectra suggested the way of separating data into mesoscale and turbulent variables independently. This approach allowed constructing similarity models of fluxes and other variables for thermodynamic and surface conditions, which considered as unfit for previous scaling.

Obtained vertical profiles of turbulent and mesoscale variables (variances and fluxes) demonstrated different behaviour. Turbulent profiles of the fluxes decreased with the height almost hyperbolic decay. All of the profiles had sharp inflections in the middle part of the CBL. This allowed us to suggest that there were two kinds of mesoscale motions in the CBL over the non-homogeneous land surface. It was supposed that mesoscale motions developed from two directions, one caused by the effect of the thermally heterogeneous surface, the influence of which extended from the surface to the middle of the CBL, and the other reflecting entrainment of the CBL with the free atmosphere or the zone above the MTIBL.

References

Albertson, J.D. and M.B. Parlange, Natural integration of scalar fluxes from complex terrain. *Advances in Water Resour.*, **23**, 239 – 252, 1999.

Hiyama, T., M.A. Strunin, R. Suzuki, J. Asanuma, M.Y. Mezrin, N.A. Bezrukova, and T. Ohata, Aircraft observations of the atmospheric boundary layer over a heterogeneous surface in Eastern Siberia. *Hydrol. Proc.*, **17**, 2885 – 2911, 2003.

Hudgins, L.H., M.E. Mayer, C.A. Frieche, Fourier and wavelet analysis of atmospheric turbulence, in "*Progress in Wavelet Analysis and Applications, Meyer Y. and S. Roques* (*eds.*)", Editions Frontiers, 491 – 498, 1993.

Kaimal J.C. and J.J. Finnigan, *Atmospheric Boundary Layer Flows, Their Structure and Measurements.* Oxford Univ. Press, New York, Oxford, 289 pp, 1994.

Sorbjan, Z., Evaluation of local similarity functions in the convective boundary layer, *Boundary-Layer Meteorol.*, **30**, 1565 – 1583, 1991.

Strunin, M.A., T. Hiyama, J. Asanuma, and T. Ohata, Aircraft observations of the development of thermal internal boundary layers and scaling of the convective boundary layer over non-homogeneous land surfaces. *Boundary-Layer Meteorol.*, **111**, 491 – 522, 2004.

Strunin, M.A. and T. Hiyama, Applying wavelet transforms to analyze aircraft-measured turbulence and turbulent fluxes in the atmospheric boundary layer over Eastern Siberia. *Hydrol. Proc.*, 2004 (in press).